

## A new method of calculating the running coupling constant \*

---

**Erek Bilgici<sup>a</sup>, Antonino Flachi<sup>b</sup>, Etsuko Itou<sup>b,†</sup>, Masafumi Kurachi<sup>b,†</sup>,  
C.-J David Lin<sup>c,d</sup>, Hideo Matsufuru<sup>e</sup>, Hiroshi Ohki<sup>b,f</sup>, Tetsuya Onogi<sup>b</sup>  
and Takeshi Yamazaki<sup>b</sup>**

(a) *Institut für Physik, Universität Graz, A-8010 Graz, Austria*

(b) *Yukawa Institute for Theoretical Physics, Kyoto University, Kyoto 606-8502, Japan*

(c) *Institute of Physics, National Chiao-Tung University, Hsinchu 300, Taiwan*

(d) *Physics Division, National Centre for Theoretical Sciences, Hsinchu 300, Taiwan*

(e) *High Energy Accelerator Research Organization (KEK), Tsukuba 305-0801, Japan*

(f) *Department of Physics, Kyoto University, Kyoto 606-8501, Japan*

<sup>†</sup> *speaker*

*E-mail:* itou@yukawa.kyoto-u.ac.jp, kurachi@yukawa.kyoto-u.ac.jp

We propose a new method to compute the running coupling constant of gauge theories on the lattice. We first give the definition of the running coupling in the new scheme using the Wilson loops in a finite volume, and explain how the running of the coupling constant is extracted from the measurement of the volume dependence. The perturbative calculation of the renormalization constant to define the scheme is also given at the leading order. As a benchmark test of the new scheme we apply the method the case of the quenched QCD. We show the preliminary result from our numerical simulations which are carried out with plaquette gauge action for various lattice sizes and bare lattice couplings. With techniques to improve the statistical accuracy, we show that we can determine the non-perturbative running of the coupling constant in a wide range of the energy scale with relatively small number of gauge configurations in our scheme. We compare our lattice data of the running coupling constant with perturbative renormalization group evolution at one- and two-loop order, and confirm the consistency between them at high energy.

*The XXVI International Symposium on Lattice Field Theory*

*July 14 - 19, 2008*

*Williamsburg, Virginia, USA*

*Report number: YITP-08-68*

---

\*Based on the contributions of E. Itou and M. Kurachi

## 1. Introduction

The properties of a vectorial gauge theory which has (near) conformal infrared fixed point (IRFP) are of fundamental importance. In addition to its intrinsic field-theoretic interest, this approximate conformal, or “walking”, behavior is an essential ingredient of modern technicolor models of dynamical electroweak symmetry breaking [1], providing requisite enhancement of Standard Model fermion masses [2, 3, 4, 5, 6, 7]. This walking behavior could also give a remedy for the problem of large correction (often denoted as  $S$  [8, 9]) to the  $Z$  boson propagator [10, 11, 12]. Our ultimate objective is to investigate the nature of physics in such a near conformal gauge theory. However, we first have to address the following question: is there any theory which actually has a conformal nature in a certain energy region?

An  $SU(N)$  gauge theory with a large number of massless fermions has been known as a promising candidate for a theory which has the nontrivial IRFP [13]. For example, in the case of  $SU(3)$  gauge theory, when the number of massless fermions,  $N_f$ , takes values in the range  $8 < N_f \leq 16$ , the two-loop running coupling approaches to a finite value,  $\alpha_* = \frac{4\pi(33/2 - N_f)}{19(N_f - 153/19)}$ , in the infrared energy region due to the existence of the IRFP. When  $N_f$  is close to 16 (which is the largest  $N_f$  we can take when we restrict our study to asymptotically free theories), even though the value of  $\alpha_*$  is corrected by higher order terms in the perturbative expansion, the existence of the IRFP is valid beyond two-loop approximation since the coupling is small enough. However, when we consider a range of  $N_f$  where the above two-loop estimation of  $\alpha_*$  becomes large, it is quite non-trivial whether this IRFP really exists beyond perturbation theory.

In principle, lattice simulations should provide a way to determine whether an  $SU(N)$  gauge theory with a certain number of massless fermions has conformal fixed point or not. Several pioneering works [14] found the chiral phase transition at certain critical flavor, which can be considered as an indication of the appearance of the IRFP. However, groups that have studied this have not reached consensus on the critical number of flavor for the chiral phase transition. Recently, Appelquist et al. [15] directly calculated the running coupling of the  $SU(3)$  gauge theory with 8 and 12 flavors by using the Schrödinger functional (SF) method on the lattice, and showed an evidence for the existence of the IRFP for  $N_f = 12$  while the running coupling for  $N_f = 8$  is more like QCD with three flavors.

Here, we propose a new scheme for the calculation of the running coupling on the lattice. We extract the renormalized coupling from the Wilson loops in a finite volume, and determine the running of the coupling constant from the measurement of the volume dependence by using the step scaling procedure. This new scheme can serve as an alternative computational method in general gauge theories.

In the context of exploring the conformal window, using a different scheme to calculate the coupling constant is well-motivated by itself to verify the real existence of the fixed point. Technical advantage of our scheme is that it is free from  $O(a)$  error in contrast to the SF scheme, in which it is practically difficult to remove all the  $O(a)$  discretization effects.

In Section 2, we define the new scheme for the determination of the running coupling. Then we review the step-scaling procedure to show how to actually obtain the evolution of the running coupling from lattice simulations in Section 3. Sections 4 and 5 are devoted to the explanation of the details of our numerical simulations, and in Section 6, we show the result of the quenched

study as a test to see the effectiveness of our new scheme for the calculation of the running coupling. Discussion on the numerical results are also given in Section 6. Section 7 summarizes our conclusions.

## 2. Wilson Loop Scheme

In this section, we give the definition of the new renormalization scheme, the ‘‘Wilson loop scheme’’, for the running coupling, and show how to calculate it on the lattice. Let us start with general features in the renormalization of the coupling constant. Consider an amplitude  $A$  whose tree-level contribution is proportional to  $g_0^2$  (where  $g_0$  is the bare coupling constant):

$$A^{\text{tree}} = k g_0^2. \quad (2.1)$$

Here,  $k$  is a certain coefficient which is a function of all the parameters of the theory except  $g_0$ . Then, we denote the ratio of the fully non-perturbative value of the amplitude  $A$  to its tree-level value as  $Z(\mu)$ :

$$A^{\text{NP}}(\mu) = Z(\mu) A^{\text{tree}}, \quad (2.2)$$

where  $\mu$  is the scale at which the amplitude  $A$  is defined. By using Eq. (2.1), the right hand side of the above equation can be rewritten as  $Z(\mu) g_0^2 k$ , and the combination  $Z(\mu) g_0^2$  can be identified as the renormalized coupling at the scale  $\mu$ . So the renormalized coupling,  $g(\mu)$ , can be expressed as follows:

$$g^2(\mu) = \frac{A^{\text{NP}}(\mu)}{k}. \quad (2.3)$$

Thus, any amplitude with a tree-level value proportional to  $g_0^2$  can be used to define the renormalized coupling. Here, we use the following quantity:

$$-R^2 \frac{\partial^2}{\partial R \partial T} \ln \langle W(R, T; L_0, T_0) \rangle \Big|_{T=R}, \quad (2.4)$$

where  $W(R, T)$  is the Wilson loop. The definition of the Wilson loop is graphically shown in Fig. 1. In this figure,  $T_0$ ,  $L_0$ , and  $T$ ,  $R$  represent the size of the box and the Wilson loop in the temporal and spatial directions, respectively, and  $a$  is the lattice spacing. From now on, for simplicity, we consider the case of  $T_0 = L_0$ . At tree level in the perturbative expansion, this quantity actually is proportional to  $g_0^2$ , *i.e.*,

$$-R^2 \frac{\partial^2}{\partial R \partial T} \ln \langle W(R, T; L_0) \rangle^{\text{tree}} \Big|_{T=R} = k g_0^2, \quad (2.5)$$

where  $k$ , in the case of periodic boundary condition for example, is

$$k = -R^2 \frac{\partial^2}{\partial R \partial T} \left[ \frac{4}{(2\pi)^4} \sum_{n_0, n_1, n_2, n_3 (\neq 0)} \left( \frac{\sin(\frac{\pi n_0 T}{L_0})}{n_0} \right)^2 \frac{e^{i \frac{2\pi n_1 R}{L_0}}}{n_0^2 + \vec{n}^2} \right]_{T=R} + \text{zero mode contribution}. \quad (2.6)$$

Here,  $(n_0, n_1, n_2, n_3)$  represents integer four-vector to define the momentum. ‘‘Zero mode contribution’’ in the above equation is coming from the existence of so-called ‘‘toron’’ contributions which

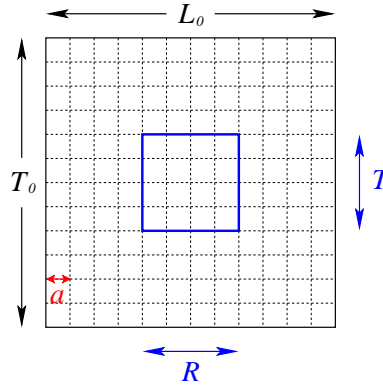


**Figure 1:** Wilson loop defined on the latticized space-time box.  $T_0$ ,  $L_0$  and  $T$ ,  $R$  represent the size of the box and the Wilson loop in the temporal and spatial directions, respectively.  $a$  is the lattice spacing.

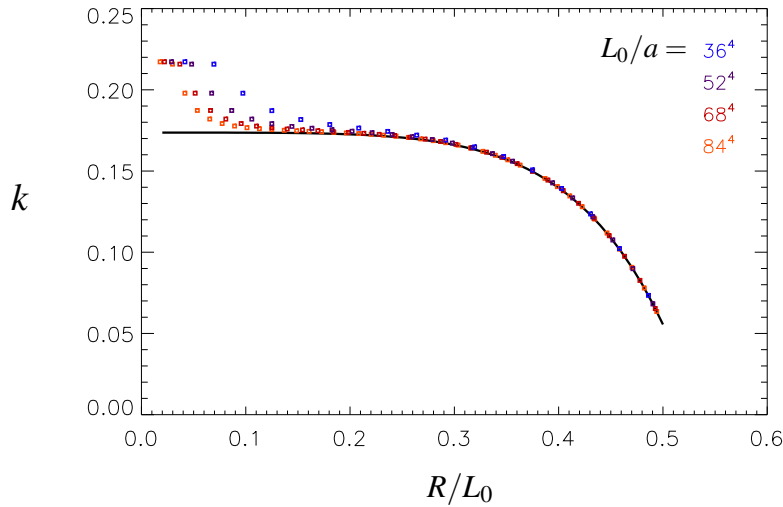


**Figure 2:** Values of  $k$  for several values of  $R/L_0$  and  $L_0/a$  (colored squares whose  $L_0/a$  is indicated by the numbers with the same color). The value of  $k$  in the continuum limit is also shown as a solid curve.

originate from zero-mode configurations degenerate with the vacuum on the periodic torus. This contribution is calculated in Ref. [16], and we use the result from that paper. After evaluating the summation in Eq. (2.6)<sup>1</sup>, one can find that  $k$  only depends on the value of  $R/L_0$ . The value of  $k$  as a function of  $R/L_0$  in the continuum limit is shown in Fig. 2. We also did similar calculations of  $k$  in the case of discrete space-time, and plotted them for several values of  $L_0/a$  and  $R/L_0$ . Note that the continuum limit actually exists (*i.e.*,  $k$  is finite in the limit of  $L_0/a \rightarrow \infty$ ) and that the convergence to continuum value is faster for larger values of  $R/L_0$ . Once the value of  $k$  is obtained, the

<sup>1</sup>Detailed calculation of the factor  $k$  can be found in [17].

renormalized coupling is defined according to Eq. (2.3):

$$g^2\left(L_0, \frac{R}{L_0}\right) = \frac{-R^2 \frac{\partial^2}{\partial R \partial T} \ln \langle W(R, T; L_0) \rangle^{\text{NP}} \Big|_{T=R}}{k\left(\frac{R}{L_0}\right)}. \quad (2.7)$$

The numerator on the right hand side of Eq. (2.7) can be estimated from the Creutz ratio on the lattice,

$$\chi(\hat{R} + 1/2, \hat{T} + 1/2; L_0/a) = -\ln \left( \frac{W(\hat{R} + 1, \hat{T} + 1; L_0/a) W(\hat{R}, \hat{T}; L_0/a)}{W(\hat{R} + 1, \hat{T}; L_0/a) W(\hat{R}, \hat{T} + 1; L_0/a)} \right), \quad (2.8)$$

where  $\hat{T} \equiv T/a$  and  $\hat{R} \equiv R/a$ . The value of  $\chi$  is evaluated by a Monte Carlo (MC) simulation. Then the renormalized coupling constant in the Wilson loop scheme can be written as:

$$g_w^2\left(L_0, \frac{R+a/2}{L_0}, \frac{a}{L_0}\right) = (\hat{R} + 1/2)^2 \cdot \chi(\hat{R} + 1/2; L_0/a)/k, \quad (2.9)$$

where we used the shorthand notation  $\chi(\hat{R} + 1/2, \hat{T} + 1/2; L_0/a)|_{\hat{R}=\hat{T}} \equiv \chi(\hat{R} + 1/2; L_0/a)$ . Here, since  $g_w^2$  depends on three different scales, namely,  $L_0$ ,  $R$ , and  $a$ , we indicated that  $g_w^2$  can be viewed as a function of  $L_0$ ,  $(R + a/2)/L_0 (\equiv r)$ , and  $a/L_0$ . We choose a specific value of  $r$  ( $r = 0.3$ , for example) and keep it fixed to that value throughout the analysis. Varying  $r$  means changing renormalization scheme. As for  $a/L_0$ , we extrapolate it to zero when taking the continuum limit. After fixing these two dimensionless parameters  $r$  and  $a/L_0$ ,  $g_w^2$  becomes a function of only one scale,  $L_0$ . In our scheme,  $L_0$  is identified as the scale at which the renormalized coupling is defined.

One thing we should emphasize here is that the Creutz ratio is free from  $O(a)$  discretization error, mainly because  $O(a)$ -improvement of the heavy quark propagator is automatically achieved after the redefinition of the mass and the wavefunction [18]. Thus, our scheme explained here does not have any  $O(a)$  systematic error as long as we use actions which do not have  $O(a)$  error.

### 3. Step scaling

Here, we review the step-scaling procedure [19, 20] in the Wilson loop scheme, which enables us to evaluate the evolution of the running coupling for a large range of energy scale on the lattice. First, we choose a specific value for  $g_w^2$ ,  $g_w^2 = \tilde{g}_w^2$ . Then, for a fixed value of  $r$ , we find sets of parameters,  $(\beta, L_0/a)$ , which reproduce  $\tilde{g}_w^2$  for several different values of  $L_0/a$ :

$$\left\{ \left( \beta_1^{(1)}, (L_0/a)_1^{(1)} \right), \left( \beta_2^{(1)}, (L_0/a)_2^{(1)} \right), \dots \right\}. \quad (3.1)$$

What we are doing here is tuning the value of  $\beta$  in such a way that the physical volume  $L_0$  is fixed for different values of  $L_0/a$ . Let us call this fixed physical volume for the starting point as  $\tilde{L}_0$ , *i.e.*,  $g_w^2(\tilde{L}_0) = \tilde{g}_w^2$ . Next thing to do is to vary the physical volume from  $\tilde{L}_0$  to  $s\tilde{L}_0$ , which gives the evolution of the running coupling from the energy scale  $1/\tilde{L}_0$  to  $1/s\tilde{L}_0$ . Here  $s$  is the scaling factor. This step can be achieved by changing the lattice size from  $(L_0/a)^{(1)}$  to  $s(L_0/a)^{(1)}$  with each value of  $\beta^{(1)}$  unchanged. Values of  $g_w^2$  calculated with these new parameter sets should be

considered as the coupling at the energy scale  $1/s\tilde{L}_0$  up to discretization error, so the extrapolation to the continuum limit can be taken by using those data.

$$g_R^2\left(\frac{1}{s\tilde{L}_0}\right) \equiv \lim_{a \rightarrow 0} \left[ Z\left(\frac{1}{s\tilde{L}_0}, \frac{a}{s\tilde{L}_0}\right) g_0^2(a) \right]. \quad (3.2)$$

The resultant value of coupling,  $g_R^2$ , should be considered as the renormalized coupling at the energy scale  $1/s\tilde{L}_0$ . This is the way to obtain a single discrete step of evolution of the running coupling with the scaling factor  $s$ .

Next, we find new parameter sets of  $(\beta^{(2)}, (L_0/a)^{(2)})$  which reproduce the value of  $g_w^2(s\tilde{L}_0)$  obtained in the previous step. Here, we find these parameter sets in such a way that the new lattice size  $L_0/a^{(2)}$  is equal to the original small lattice  $(L_0/a)^{(1)}$ . From here, we can repeat exactly the same procedure as that of the first step scaling explained in the previous paragraph: we calculate  $g_w^2$  with the parameter sets  $(\beta^{(2)}, s(L_0/a)^{(1)})$ . By iterating this procedure, say,  $n$  times, we obtain the evolution of the running coupling from the energy scale  $1/\tilde{L}_0$  to  $1/(s^n\tilde{L}_0)$ .

In our exploratory study, we slightly modify the step scaling procedure. Instead of tuning  $\beta$  to keep  $g_w^2(\tilde{L}_0)$  fixed, we use the results given by Alpha collaboration [21], namely, we use the parameter sets which are tuned to keep the renormalized coupling in the SF scheme,  $g_{SF}^2(\tilde{L}_0)$ , fixed. We also use the result given in [22] to obtain additional parameters for the study of lower energy region.

#### 4. Simulation parameters

We consider a four-dimensional Euclidean lattice  $L_0^4$ . In this work, we use the standard Wilson plaquette gauge action. Gauge configurations are generated by the pseudo-heatbath algorithm and over-relaxation, mixed in the ratio of 1:5. We call the combination of one pseudo-heatbath update sweep followed by five over-relaxation sweeps ‘‘an iteration’’. In order to ensure decorrelation, we save gauge configurations separately by 1000 iterations and perform measurements on them. The number of gauge configurations we generated is 100 at each set of  $(\beta, L_0/a)$ . We use both periodic and twisted boundary conditions. However, in this article we only report the case of periodic boundary condition.

We have five parameter sets (Set 1- Set 5) of  $(\beta, L_0/a)$  corresponding to the fixed physical box size  $L_0$  as in Table 1.

The values of  $\beta$  for Set 1-4 are tuned by fixing  $L_0$  using the renormalized coupling in SF scheme,  $g_{SF}^2$ , as inputs. (See, Table 6 in [21].) Also, these parameters are tuned in such a way that the value of  $g_{SF}^2$  obtained from the first column (*i.e.*  $s = 1$ ) of Set 2 (or 3, 4) coincide with that obtained from the second column (*i.e.*  $s = 2$ ) of Set 1 (or 2, 3) up to systematic and statistical errors. Thus, if we call the energy scale defined by the  $s = 1$  of Set 1 as  $1/\tilde{L}_0$ , from the simulations with parameters in Set 1-4, we obtain the evolution of the running coupling from  $1/\tilde{L}_0$  to  $1/(2^4\tilde{L}_0)$ . We also added an extra set (Set 5) of parameters to obtain further step scalings toward low energy region. Parameters in Set 5 are tuned by using the Sommer scale,  $r_0$ , as inputs. (See Eq. (2.18) in [22].)

Note that even though we use existing parameter sets which are tuned by using  $g_{SF}^2$  or  $r_0$  as an input here, to make our study self-contained, we should tune parameters by using  $g_w^2$  itself. Such study is underway, and will be presented in our future publication [17].

Set 1			Set 2			Set 3			Set 4		
$\beta$	$L_0/a$ ( $s=1$ )	$L_0/a$ ( $s=2$ )	$\beta$	$L_0/a$ ( $s=1$ )	$L_0/a$ ( $s=2$ )	$\beta$	$L_0/a$ ( $s=1$ )	$L_0/a$ ( $s=2$ )	$\beta$	$L_0/a$ ( $s=1$ )	$L_0/a$ ( $s=2$ )
8.2500	(8)	16	7.6547	(8)	16	7.0197	(8)	16	6.4527	(8)	16
8.4677	(10)	20	7.8500	(10)	20	7.2098	(10)	20	6.6629	(10)	20
8.5985	12	24	7.9993	12	24	7.3551	12	24	6.7750	12	24
8.7289	14		8.1352	14		7.4986	14		6.9169	14	
8.8323	16		8.2415	16		7.0203	16		7.6101	16	

Set 5			
$\beta$	$L_0/a$ ( $s=1$ )	$L_0/a$ ( $s=1.5$ )	$L_0/a$ ( $s=2$ )
6.1274	(8)	12	16
6.2647	(10)		20
6.3831	12	18	24
6.4841	14		
6.5700	16	24	

**Table 1:** The parameter sets of  $\beta$  and  $L_0/a$  used for measurements. Each of the first columns in Sets 1-4 gives the constant SF coupling, and the first one in Set 5 gives the constant Sommer scale. The parameter sets of  $L_0/a = 8$  and 10 (denoted by parentheses) are used only for the reference to set the scale, but not for measurements.

## 5. Simulation details

Now, we calculate the renormalized coupling constant in the Wilson loop scheme defined by Eq. (2.9) for a fixed value of  $r$ :

$$g_w^2(L_0, a/L_0) = (\hat{R}^2 + 1/2)^2 \cdot \chi(\hat{R} + 1/2; L_0/a) / k|_{\text{fixed } r}. \quad (5.1)$$

First, to reduce the statistical error, we use the APE smearing [23] of link variables defined by the following equation;

$$U_{x,\mu}^{(n+1)} = Proj_{SU(3)} \left[ U_{x,\mu}^{(n)} + \frac{1}{c} \sum_{\mu \neq \nu}^4 U_{x,\nu}^{(n)} U_{x+\nu,\mu}^{(n)} U_{x+\mu,\nu}^{(n)\dagger} \right], \quad (5.2)$$

where  $n$  and  $c$  denote a smearing level and a smearing parameter, respectively. The result does not depend on the value of  $c$  significantly, and we take  $c = 2.3$  in this work. Note that we need to find an optimal set of  $r \equiv \frac{R+a/2}{L_0}$  and the smearing level  $n$  by considering the following requirements. To control the discretization error, it is better to choose a larger  $r$ . For the purpose of reducing the statistical error, it is better to take a smaller  $r$  and higher  $n$ . Fig. 3 shows the smearing-level dependence of  $(\hat{R} + 1/2)^2 \cdot \chi$  in the case of  $\beta = 6.3831$  and  $L_0/a = 18$  as an example. From this figure, we find the statistical error is notably reduced even at smearing level one. Furthermore,

in order to avoid over-smearing,  $n$  should be smaller than  $\hat{R}/2$ . This condition gives the lower bound,  $L_0/a > (4n+1)/2$ . We summarize the bound from this requirement in Table 2. We actually see, for example in the case of  $L_0/a = 18$  (see Fig. 3), that the data of  $(\hat{R} + 1/2) = 1.5, 2.5$  in higher smearing level are not reliable because of over-smearing. By considering all of the above requirements, we find that  $(r, n) = (0.3, 1)$  is an optimal choice.

$$(\hat{R} + 1/2)^2 \cdot \chi$$

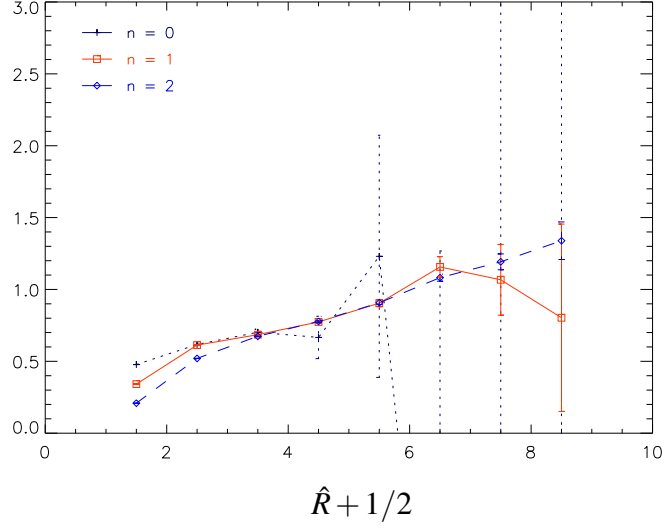


**Figure 3:** The values of  $(\hat{R} + 1/2)^2 \cdot \chi$  with statistical error for several  $(\hat{R} + 1/2)$  in the case of  $\beta = 6.3831$  and  $L_0/a = 18$ . The black cross, the red square and the blue diamond denote the data with 0, 1 and 2 smearing, respectively.

$n$	$r = 0.25$	$r = 0.30$	$r = 0.35$
$n = 1$	$L_0/a > 10$	$L_0/a > 8.3$	$L_0/a > 7.1$
$n = 2$	$L_0/a > 18$	$L_0/a > 15$	$L_0/a > 12.8$
$n = 3$	$L_0/a > 26$	$L_0/a > 21.6$	$L_0/a > 18.5$

**Table 2:** The lower bound for  $L_0/a$  to avoid over smearing.

From here, we fix the renormalization condition  $r = 0.3$ , then we have to calculate the value of  $(\hat{R} + 1/2)^2 \cdot \chi$  for noninteger  $\hat{R}$ . We interpolate the value of  $(\hat{R} + 1/2)^2 \cdot \chi$  using a quadratic fit function:

$$f(\hat{R} + 1/2) = c_0 + c_1(\hat{R} + 1/2) + c_2(\hat{R} + 1/2)^2. \quad (5.3)$$

We determine the fit ranges for each lattice size as in Table 3. We confirmed that the data can be well fitted by our fit function with these fit ranges for all parameter sets. An example is shown in Fig. 4.

Finally, we take the continuum limit of the running coupling constant of each column in Table 1. We show the example of the extrapolation of the coupling constant in Fig. 5. The red line

$L_0/a$	$\hat{R} + 1/2$	$\hat{R}_{min}$	$\hat{R}_{max}$
12	3.6	2	4
14	4.2	2	5
16	4.8	3	5
18	5.4	4	6
20	6.0	4	6
24	7.2	5	7

**Table 3:** The fit range used to interpolate the value of  $(\hat{R} + 1/2)^2 \cdot \chi$ . The column “ $\hat{R} + 1/2$ ” is the value that corresponds to  $r = 0.3$ .

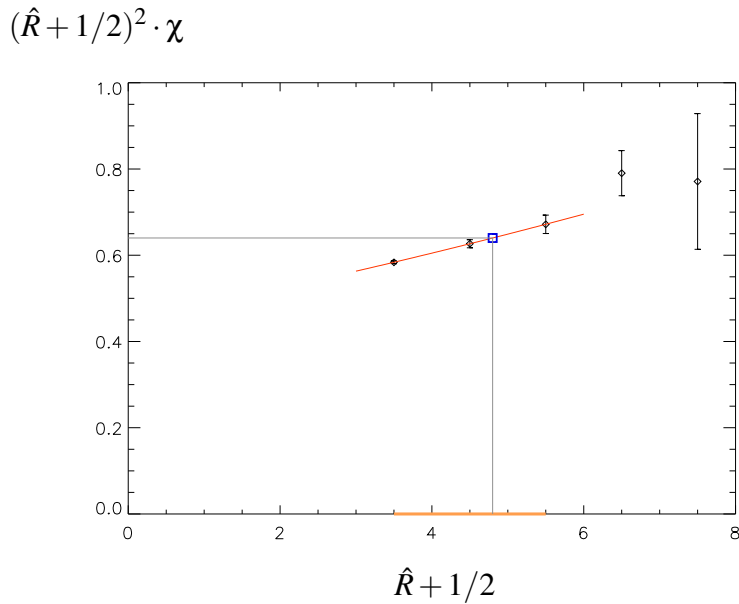


**Figure 4:** The plot for the interpolation of  $(\hat{R} + 1/2)^2 \cdot \chi$  in the case of  $\beta = 6.5700$  and  $L_0/a = 16$ . The diamonds show the resultant values of  $(\hat{R} + 1/2)^2 \cdot \chi$  for integer  $\hat{R}$  with statistical error. The red line represents the function  $f(\hat{R} + 1/2)$  fitted to the data in the range of  $3 \leq \hat{R} \leq 5$ . The blue box indicates the interpolated value corresponding to  $r = 0.3$ .

corresponds to the extrapolation of the first column of Set 1, and the blue line is that of the second column of Set 1. The values at the continuum limit are the renormalized coupling constants at scales  $1/\bar{L}_0$  and  $1/(2\bar{L}_0)$ , respectively. In performing the continuum extrapolation, we have used the fit function linear in  $(a/L_0)^2$ :

$$c_0 + c_1 \left( \frac{a}{L_0} \right)^2. \quad (5.4)$$

As explained in section 2, our Wilson loop scheme does not have  $O(a)$  systematic error. However, in the present quenched QCD test, since we took the SF coupling, which has  $O(a)$  error, as a constant input parameter, it is possible that an  $O(a)$  error is introduced also in our data. Fig. 5 shows that the data are nicely fitted by the linear function, Eq. (5.4). This would indicate that

$O(a)$  systematic error and possible higher order discretization error are small as we expected from perturbative analysis [24] in this weak coupling regime.

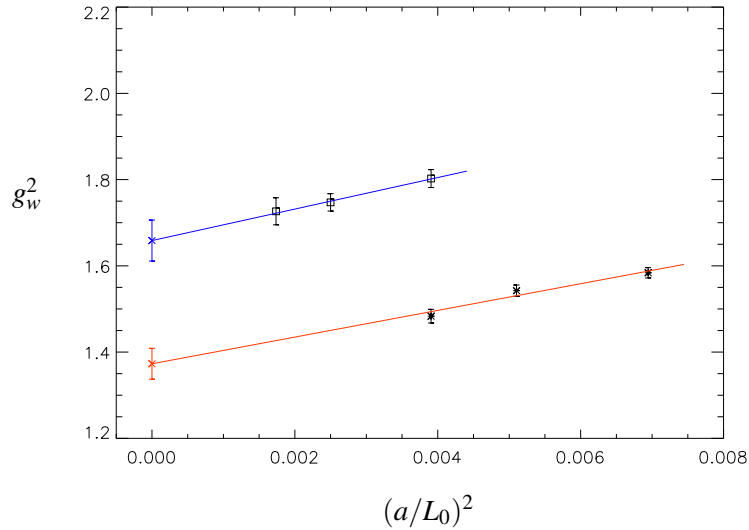


**Figure 5:** The continuum limit of  $g_w^2$  in Set 1. The red and blue lines describe the continuum limit of the first and second columns of Set 1, respectively.

## 6. Results and discussion

We plot the numerical results for the energy scale dependence of the renormalized coupling in the Wilson loop scheme in Fig. 6. The perturbative renormalization group evolution at one-loop and two-loop are also displayed in the figure for comparison. Our MC data are consistent with the perturbative results in high energy region, while there is difference in low energy region because of the higher loop or the nonperturbative effect.

Recall that the second column ( $s = 2$ ) of Set 1 (or 2, 3, 4) and the first column ( $s = 1$ ) of Set 2 (or 3, 4, 5) in Table 1 give the same value of the renormalized coupling in the SF scheme within the statistical error. From Fig. 6, we see that our results in the Wilson loop scheme also show that the step scaling procedure works well; steps are nicely connected as in the case of the SF couplings. It suggests that the systematic errors, such as the interpolation in  $\hat{R} + 1/2$ ,  $O(a)$  error in SF coupling and the extrapolation to the continuum limit are under control. To make our study self-contained, we should extend this scheme by taking  $g_w^2$ , which has no  $O(a)$  systematic error, as an input physical parameter. Such study is underway, and will be presented in our future publication [17].

Finally, we emphasize that there is an optimal choice of smearing level and  $r$  with which both the statistical and discretization errors are under control. The number of gauge configurations we used for the present study was only 100 for each  $(\beta, L_0/a)$ . From this small number of gauge configurations, we obtained data with a few ( $\sim 10$ ) percent statistical error in high (low) energy region. Thus, we could expect that this scheme is promising for the study of other theories.

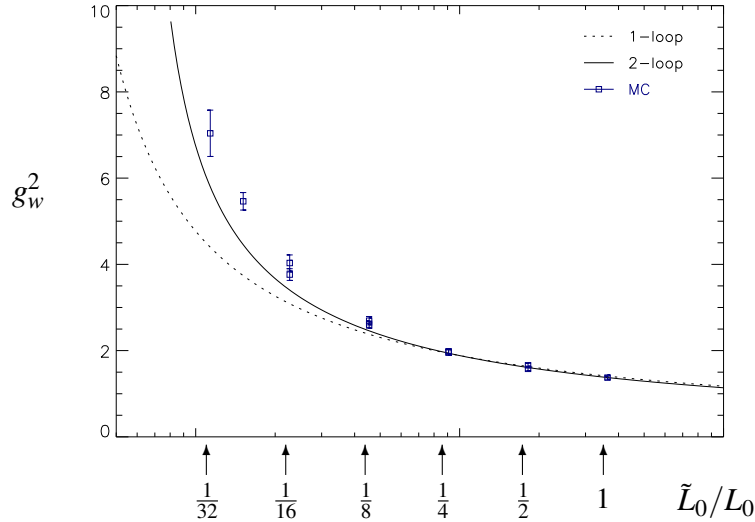


**Figure 6:** The running coupling in the Wilson loop scheme. The horizontal axis is the ratio of the energy scale  $\tilde{L}_0/L_0$ , and the vertical axis is the renormalized coupling in the Wilson loop scheme. The square symbols indicate our lattice data of the running coupling constants. The right-most symbol corresponds to the renormalized coupling given by the first column of Set 1 at scale  $1/\tilde{L}_0$ , the adjacent two overlapping symbols give the couplings from the second column of Set 1 and the first column of Set 2 at scale  $1/(2\tilde{L}_0)$ , and similarly for the remaining data for lower energy scales. The perturbative running couplings at one-loop (dotted line) and two-loop (solid line) are also shown for comparison.

## 7. Summary

We proposed a new scheme for the determination of the running coupling on the lattice. Our method is based on the measurement of the finite volume dependence of the Wilson loop. Unlike the SF scheme, our method does not have any  $O(a)$  discretization error, therefore the systematic error arising from the extrapolation to the continuum limit is expected to be quite small. We showed results of preliminary numerical study for the quenched QCD as a feasibility test of our scheme, and confirmed that the method actually reproduced the step scaling of the coupling which is consistent with the two-loop running coupling at high energy. We also showed that the coupling calculated by this newly proposed scheme deviates from that with two-loop approximation below a certain energy scale. This deviation arises from the effects that are not captured by the two-loop approximation. We have confirmed that our scheme works well for the calculation of the running coupling with relatively small number of gauge configurations, via demonstrating that the statistical error is under control by properly choosing the smearing level and  $r$ . We expect that this new method is quite useful to calculate the running coupling of the  $SU(N)$  gauge theory with a large number of dynamical fermions, which will be studied in our future work.

The properties of a vectorial gauge theory as a function of the number of fermions is quite interesting. Through the analyses based on the Schwinger-Dyson and Bethe-Salpeter equations, it is shown that there is chiral symmetry restoration at certain critical number of fermions [5, 7], and that the behavior of the meson spectrum, the  $S$  parameter, *etc.*, are quite different from those in

QCD with three flavors. [11, 12, 25, 26]. In these analyses, two-loop running coupling was used as an approximation to the fully non-perturbative vertices. Therefore, the existence of the IRFP is an assumption and an input in these analyses. The confirmation of the existence of the IRFP by lattice simulations justifies this assumption, and motivates a fully non-perturbative study of near conformal gauge theories on the lattice.

## Acknowledgment

This work is supported in part by the Grant-in-Aid of the Ministry of Education (Nos. 19540286, 19740160 and 20039005). E. B. is supported by the FWF Doktoratskolleg Hadrons in Vacuum, Nuclei and Stars (DK W1203-N08). A. F. acknowledges the support of JSPS, Grant N.19GS0210. C.-J D. L. is supported by the National Science Council of Taiwan via grant number 96-2112-M-009-020-MY3. H. O. thanks N. Yamada for his support, especially by Grand-in-Aid for Scientific Research No. 20025010 from the Ministry of Education, Culture, Sports, Science and Technology of Japan. T.Y. is the Yukawa Fellow supported by Yukawa Memorial Foundation. Numerical simulation was carried out on the vector supercomputer NEC SX-8 in YITP, Kyoto University.

## References

- [1] S. Weinberg, Phys. Rev. D **19**, 1277 (1979); L. Susskind, *ibid.* D **20**, 2619 (1979); see also S. Weinberg, Phys. Rev. D **13**, 974 (1976).
- [2] B. Holdom, Phys. Lett. B **150**, 301 (1985).
- [3] K. Yamawaki, M. Bando, and K. Matumoto, Phys. Rev. Lett. **56**, 1335 (1986).
- [4] T. Appelquist, D. Karabali, and L. C. R. Wijewardhana, Phys. Rev. Lett. **57**, 957 (1986); T. Appelquist and L. C. R. Wijewardhana, Phys. Rev. D **35**, 774 (1987); Phys. Rev. D **36**, 568 (1987).
- [5] T. Appelquist, J. Terning, and L. C. R. Wijewardhana, Phys. Rev. Lett. **77**, 1214 (1996).
- [6] V. Miransky and K. Yamawaki, Phys. Rev. D **55**, 5051 (1997); *ibid.* **56**, E 3768 (1997). See also V. Miransky and P. Fomin, Sov. J. Part. Nucl. **16**, 203 (1985).
- [7] T. Appelquist, A. Ratnaweera, J. Terning, and L. C. R. Wijewardhana, Phys. Rev. D **58**, 105017 (1998).
- [8] M. E. Peskin and T. Takeuchi, Phys. Rev. Lett. **65**, 964 (1990); Phys. Rev. D **46**, 381 (1992).
- [9] G. Altarelli and R. Barbieri, Phys. Lett. B **253**, 161 (1991); G. Altarelli, R. Barbieri, F. Caravaglios, Int. J. Mod. Phys. A **13**, 1031 (1998).
- [10] T. Appelquist and F. Sannino, Phys. Rev. D **59**, 067702 (1999).
- [11] M. Harada, M. Kurachi and K. Yamawaki, Prog. Theor. Phys. **115**, 765 (2006).
- [12] M. Kurachi and R. Shrock, Phys. Rev. D **74**, 056003 (2006).
- [13] An early paper on the phase structure of vectorial gauge theories is T. Banks and A. Zaks, Nucl. Phys. B **196** (1982), 189; see also D. D. Dietrich and F. Sannino, Phys. Rev. D **75**, 085018 (2007), for extensive investigation of conformal window including non-fundamental representation fermions.

- [14] Y. Iwasaki et al., Phys. Rev. Lett. **69**, 21 (1992) Phys. Rev. D **69**, 014507 (2004); P. Damgaard, U. Heller, A. Krasnitz, and P. Olesen, Phys. Lett. B **400**, 169 (1997); R. Mawhinney, Nucl. Phys. B (Proc. Suppl.) **83**, 57 (2000).
- [15] T. Appelquist, G. T. Fleming and E. T. Neil, Phys. Rev. Lett. **100**, 171607 (2008).
- [16] A. Coste, A. Gonzalez-Arroyo, J. Jurkiewicz and C. P. Korthals Altes, Nucl. Phys. B **262**, 67 (1985).
- [17] E. Bilgici, A. Flachi, E. Itou, M. Kurachi, C.-J D. Lin, H. Matsufuru, H. Ohki, T. Onogi and T. Yamazaki, in preparation.
- [18] S. Necco and R. Sommer, Nucl. Phys. B **622**, 328 (2002) [arXiv:hep-lat/0108008].
- [19] M. Luscher, P. Weisz and U. Wolff, Nucl. Phys. B **359**, 221 (1991).
- [20] S. Caracciolo, R. G. Edwards, S. J. Ferreira, A. Pelissetto and A. D. Sokal, Phys. Rev. Lett. **74**, 2969 (1995).
- [21] S. Capitani, M. Luscher, R. Sommer and H. Wittig [ALPHA Collaboration], Nucl. Phys. B **544**, 669 (1999).
- [22] M. Guagnelli, J. Heitger, F. Palombi, C. Pena and A. Vladikas [ALPHA Collaboration], JHEP **0405**, 001 (2004)
- [23] M. Albanese *et al.* [APE Collaboration], Phys. Lett. B **192**, 163 (1987).
- [24] M. Luscher and P. Weisz, Nucl. Phys. B **479**, 429 (1996) [arXiv:hep-lat/9606016].
- [25] M. Harada, M. Kurachi and K. Yamawaki, Phys. Rev. D **68**, 076001 (2003).
- [26] M. Kurachi, R. Shrock and K. Yamawaki, Phys. Rev. D **76**, 035003 (2007).